Metathermotics: Nonlinear thermal responses of core-shell metamaterials

Shuai Yang, Liujun Xu, and Jiping Huang*

Department of Physics, State Key Laboratory of Surface Physics, and Key Laboratory of Micro and Nano Photonic Structures (MOE), Fudan University, Shanghai 200433, China

(Received 2 February 2019; published 29 April 2019)

Thermal metamaterials based on core-shell structures have aroused wide research interest, e.g., in thermal cloaks. However, almost all the relevant studies only discuss linear materials whose thermal conductivities are temperature-independent constants. Nonlinear materials (whose thermal conductivities depend on temperatures) have seldom been touched; however, they are important in practical applications. This situation largely results from the lack of a general theoretical framework for handling such nonlinear problems. Here we study the nonlinear responses of thermal metamaterials with a core-shell structure in two or three dimensions. By calculating the effective thermal conductivity, we derive the nonlinear modulation of a nonlinear core. Furthermore, we reveal two thermal coupling conditions, under which this nonlinear modulation can be efficiently manipulated. In particular, we reveal the phenomenon of nonlinearity enhancement. Then this theory helps us to design a kind of intelligent thermal transparency devices, which can respond to the direction of thermal fields. The theoretical results and finite-element simulations agree well with each other. This work not only offers a different mechanism to achieve nonlinearity modulation and enhancement in thermotics, but also suggests potential applications in thermal management, including illusion.

DOI: 10.1103/PhysRevE.99.042144

I. INTRODUCTION

Heat management has aroused intensive research interest due to its wide applications for human beings. One core problem of heat management is to tailor thermal conductivities effectively. Fortunately, thermal metamaterials have provided a powerful method to tailor thermal conductivities with delicately designed structures. Based on thermal metamaterials, a large amount of novel thermal phenomena have been realized, such as thermal cloaks [1–8], thermal concentrators [3,4], thermal rotators [9,10], thermal transparency [11–16], thermal camouflage [17–23], thermal bending [24–27], etc. To achieve these phenomena, the core-shell structure serves as a typical scheme. However, the existing research does not consider the nonlinear effect (nonlinear thermotics) except for some piecemeal studies [28–32]. Compared with nonlinear optics [33–38], nonlinear thermotics has attracted much less attention. This situation largely results from the lack of a general theoretical framework to handle nonlinear effects in thermotics.

To solve this problem, here we investigate the thermal properties of a core-shell structure embedded in a finite matrix. The core is nonlinear, and the shell and the matrix are linear. Here, the nonlinear core (or linear shell and matrix) means that the core (or shell and matrix) material has a temperature-dependent (or temperature-independent) thermal conductivity; in this case, the corresponding Fourier's law of thermal conduction shows a nonlinear (or linear) relation between the heat flux density and the temperature gradient, thus called "nonlinear core" (or "linear shell and matrix"). Then we establish a general theoretical framework to deal with nonlinear effects in both two and three dimensions. To achieve nonlinearity enhancement, we discuss the nonlinear modulation under two thermal coupling conditions after establishing the general theory. This is because, under thermal coupling conditions, the core property can be extended to the shell. In this way, the core nonlinearity may also be extended to the shell, which is beneficial for our purpose. Moreover, thermal coupling conditions largely simplify the mathematical form of the nonlinear modulation. Results indicate that the nonlinearity enhancement can appear under one of the coupling conditions. Further, the theory helps us to propose a kind of intelligent thermal transparency devices, which become automatically switchable to external temperatures. We also perform finite-element simulations to validate our theoretical predictions, and they agree well with each other.

II. THEORY

A. Two-dimensional case

We first consider the two-dimensional case; see Fig. 1(a). The core-shell structure is embedded in a finite square matrix with width a and temperature-independent (namely, linear) thermal conductivity κ_m. The shell with radius r_2 has an anisotropic linear thermal conductivity $\overleftrightarrow{\kappa}_s = \mathrm{diag}(\kappa_{rr}, \kappa_{\theta\theta})$ in cylindrical coordinates (r, θ). The core with radius r_1 has a temperature-dependent (i.e., nonlinear) thermal conductivity $\kappa_c(T)$ given by [32]

$$\kappa_c(T) = \kappa_c^{(0)} + \chi_c T^{\alpha}, \tag{1}$$

where $\kappa_c^{(0)}$ is the temperature-independent (or linear) part, χ_c and T, respectively, represent nonlinear coefficient and

*jphuang@fudan.edu.cn

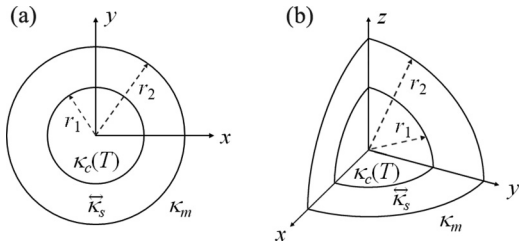

FIG. 1. Schematic diagrams of (a) two-dimensional or (b) three-dimensional core-shell structure in Cartesian coordinate system; (b) only shows one eighth of the structure for the sake of clarity. The core or shell radius is r_1 or r_2; the core, shell, and matrix have thermal conductivities of $\kappa_c(T)$, $\vec{\kappa}_s$, and κ_m, respectively. Other details can be found in the text.

temperature, and α can be any real number. We assume that the core is weakly temperature dependent (or nonlinear), say $\chi_c T^\alpha \ll \kappa_c^{(0)}$. Regarding Eq. (1), it becomes necessary for us to add two remarks as follows. On one hand, we need to point out that, in nonlinear optics, dielectric permittivities have a similar nonlinear expression because of their dependence on the electric-field component of electromagnetic waves. But, this electric field is mathematically analogous to the temperature gradient in thermotics, rather than the temperature (T) as adopted in Eq. (1). This fact implies that new physics may be expected from Eq. (1). On the other hand, Eq. (1) has realistic implications because almost all materials have temperature-dependent thermal conductivities (certainly, the dependence could be weak or strong). Particularly, thermal conductivity κ_c could increase as T either increases [39] or decreases [40].

Then, the effective thermal conductivity of the core-shell structure $\kappa_{e1}(T)$ [15] reaches

$$\kappa_{e1}(T) = u\kappa_{rr}\frac{\kappa_c(T) + u\kappa_{rr} + [\kappa_c(T) - u\kappa_{rr}]p_1^u}{\kappa_c(T) + u\kappa_{rr} - [\kappa_c(T) - u\kappa_{rr}]p_1^u}, \quad (2)$$

and that of the core-shell structure plus the matrix $\kappa_{e2}(T)$ [14] turns to be

$$\kappa_{e2}(T) = \kappa_m\frac{\kappa_{e1}(T) + \kappa_m + [\kappa_{e1}(T) - \kappa_m]p_2}{\kappa_{e1}(T) + \kappa_m - [\kappa_{e1}(T) - \kappa_m]p_2}, \quad (3)$$

where $p_1 = r_1^2/r_2^2$, $p_2 = \pi r_2^2/a^2$, and $u = \sqrt{\kappa_{\theta\theta}/\kappa_{rr}}$. The direct use of the results from Refs. [14] and [15] is valid in the paper. The reasons lie in that (i) the nonlinear term is smaller than the linear term, and thus the spatial fluctuations of the thermal conductivity are small; (ii) we assume that T is the temperature at the center of the structure. So the assumptions can average over the spatial fluctuations of the thermal conductivity. Therefore, the results from Refs. [14] and [15] are approximately valid and still contributing.

Equation (3) allows us to do Taylor expansion up to infinite terms. In the following, we keep the terms up to $T^{3\alpha}$, and neglect the other terms,

$$\kappa_{e2}(T) = \kappa_{e2}^{(0)} + \chi_e T^\alpha + \beta_e T^{2\alpha} + \gamma_e T^{3\alpha} + O(T^{4\alpha}), \quad (4)$$

where $\kappa_{e2}^{(0)}$, χ_e, β_e, and γ_e are respectively

$$\kappa_{e2}^{(0)} = \kappa_m\frac{\kappa_{e1}^{(0)} + \kappa_m + \left(\kappa_{e1}^{(0)} - \kappa_m\right)p_2}{\kappa_{e1}^{(0)} + \kappa_m - \left(\kappa_{e1}^{(0)} - \kappa_m\right)p_2}, \quad (5)$$

$$\chi_e = \frac{16u^2\kappa_{rr}^2\kappa_m^2 p_2 p_1^u \chi_c}{\left\{u\kappa_{rr}(p_2-1)\left[\kappa_c^{(0)} + u\kappa_{rr} + \left(\kappa_c^{(0)} - u\kappa_{rr}\right)p_1{}^u\right] + \kappa_m(p_2+1)\left[\kappa_c^{(0)} + u\kappa_{rr} - \left(\kappa_c^{(0)} - u\kappa_{rr}\right)p_1{}^u\right]\right\}^2}, \quad (6)$$

$$\beta_e = \frac{16u^2\kappa_{rr}^2\kappa_m^2 p_2 p_1^u \chi_c^2\left[u\kappa_{rr}\left(p_1^u+1\right)(p_2-1) + \kappa_m\left(p_1^u-1\right)(p_2+1)\right]}{\left\{u\kappa_{rr}(p_2-1)\left[\kappa_c^{(0)} + u\kappa_{rr} + \left(\kappa_c^{(0)} - u\kappa_{rr}\right)p_1{}^u\right] + \kappa_m(p_2+1)\left[\kappa_c^{(0)} + u\kappa_{rr} - \left(\kappa_c^{(0)} - u\kappa_{rr}\right)p_1{}^u\right]\right\}^3}, \quad (7)$$

$$\gamma_e = \frac{16u^2\kappa_{rr}^2\kappa_m^2 p_2 p_1^u \chi_c^3\left[u\kappa_{rr}\left(p_1^u+1\right)(p_2-1) + \kappa_m\left(p_1^u-1\right)(p_2+1)\right]^2}{\left\{u\kappa_{rr}(p_2-1)\left[\kappa_c^{(0)} + u\kappa_{rr} + \left(\kappa_c^{(0)} - u\kappa_{rr}\right)p_1{}^u\right] + \kappa_m(p_2+1)\left[\kappa_c^{(0)} + u\kappa_{rr} - \left(\kappa_c^{(0)} - u\kappa_{rr}\right)p_1{}^u\right]\right\}^4}. \quad (8)$$

Here $\kappa_{e2}^{(0)}$ is the linear part of the thermal conductivity of the core-shell structure and the matrix, and $\kappa_{e1}^{(0)} = u\kappa_{rr}[\kappa_c^{(0)} + u\kappa_{rr} + (\kappa_c^{(0)} - u\kappa_{rr})p_1^u]/[\kappa_c^{(0)} + u\kappa_{rr} - (\kappa_c^{(0)} - u\kappa_{rr})p_1^u]$ is the linear part of the thermal conductivity of the core-shell structure.

Equation (4) clearly shows that the low-order nonlinearity [Eq. (1)] can induce not only the same order nonlinearity $\chi_e T^\alpha$, but also the high-order nonlinearities (i.e., $\beta_e T^{2\alpha}$ and $\gamma_e T^{3\alpha}$). Nevertheless, owing to $\chi_c T^\alpha \ll \kappa_c^{(0)}$ in Eq. (1), it is evident to conclude that $\chi_e T^\alpha \gg \beta_e T^{2\alpha} \gg \gamma_e T^{3\alpha}$ in Eq. (4). So, in what follows, we only focus on $\chi_e T^\alpha$. To proceed, we define the nonlinear modulation $\eta = \chi_e/\chi_c$, which is given by

$$\eta = \frac{16u^2\kappa_{rr}^2\kappa_m^2 p_2 p_1^u}{\left\{u\kappa_{rr}(p_2-1)\left[\kappa_c^{(0)} + u\kappa_{rr} + \left(\kappa_c^{(0)} - u\kappa_{rr}\right)p_1{}^u\right] + \kappa_m(p_2+1)\left[\kappa_c^{(0)} + u\kappa_{rr} - \left(\kappa_c^{(0)} - u\kappa_{rr}\right)p_1{}^u\right]\right\}^2}. \quad (9)$$

This equation is the general expression of nonlinear modulation in two dimensions. Then we are allowed to discuss the nonlinear modulation η in some special cases, say, under thermal coupling conditions. Namely, when the core-shell Structure satisfies

$$\kappa_c^{(0)} + u\kappa_{rr} = 0, \quad (10)$$

$$\kappa_m = \kappa_c^{(0)}, \quad (11)$$

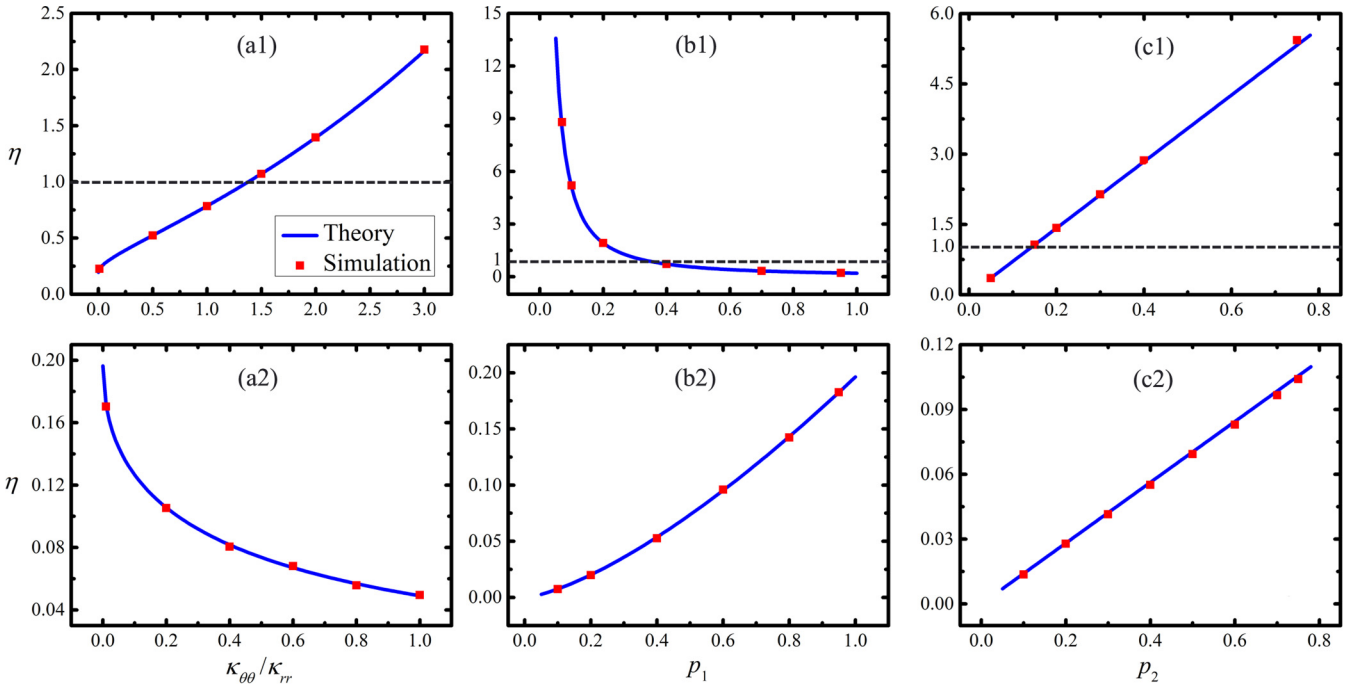

FIG. 2. Two-dimensional simulation results. (a1)–(c1) show the nonlinear modulation $\eta\ (=\chi_e/\chi_c)$ under the thermal coupling conditions determined by Eqs. (10), (11) with three variables: (a1) $\kappa_{\theta\theta}/\kappa_{rr}$, (b1) p_1, and (c1) p_2. The solid lines in (a1)–(c1) are calculated from Eq. (12), and the symbols are obtained from finite-element simulations. The solid lines in (a2)–(c2) are calculated from Eq. (15) under the thermal coupling conditions determined by Eqs. (13), (14). Other parameters: (a1), (a2) $p_1 = 0.25$ and $p_2 = \pi/16$; (b1), (b2) $\kappa_{\theta\theta}/\kappa_{rr} = 2$ and $p_2 = \pi/16$; (c1), (c2) $\kappa_{\theta\theta}/\kappa_{rr} = 2$ and $p_1 = 0.25$; (a1)–(c1) $\kappa_c(T) = 400 + 0.05T$ W/(m K), $\kappa_s = -\sqrt{\kappa_{rr}\kappa_{\theta\theta}} = -400$ W/(m K) is the effective scalar thermal conductivity, and $\kappa_m = 400$ W/(m K); (a2)–(c2) $\kappa_c(T) = 400 + 0.05T$ W/(m K), $\kappa_s = \sqrt{\kappa_{rr}\kappa_{\theta\theta}} = 400$ W/(m K), and $\kappa_m = 400$ W/(m K).

the nonlinear modulation η is simplified as

$$\eta = p_1^{-u} p_2. \tag{12}$$

On the other hand, when the core-shell structure satisfies

$$\kappa_c^{(0)} - u\kappa_{rr} = 0, \tag{13}$$

$$\kappa_m = \kappa_c^{(0)}, \tag{14}$$

the nonlinear modulation η becomes

$$\eta = p_1^{u} p_2. \tag{15}$$

Equations (10), (11) and Eqs. (13), (14) are two different thermal coupling conditions because they establish the relations among the core, shell, and matrix.

B. Three-dimensional case

The above theory can be extended to three dimensions; see Fig. 1(b). Then $\overleftrightarrow{\kappa}_s$ should be redefined as $\overleftrightarrow{\kappa}_s = \mathrm{diag}(\kappa_{rr}, \kappa_{\theta\theta}, \kappa_{\varphi\varphi})$ in spherical coordinates (r, θ, φ) with $\kappa_{\theta\theta} = \kappa_{\varphi\varphi}$ for simplicity. The effective thermal conductivity of the core-shell structure [15] in three dimensions can be expressed as

$$\kappa_{e1}(T) = \kappa_{rr}\frac{v_1[\kappa_c(T) - v_2\kappa_{rr}] - v_2[\kappa_c(T) - v_1\kappa_{rr}]p_1^w}{[\kappa_c(T) - v_2\kappa_{rr}] - [\kappa_c(T) - v_1\kappa_{rr}]p_1^w}, \tag{16}$$

and that of the core-shell structure plus the matrix [14] is

$$\kappa_{e2}(T) = \kappa_m\frac{\kappa_{e1}(T) + 2\kappa_m + 2[\kappa_{e1}(T) - \kappa_m]p_2}{\kappa_{e1}(T) + 2\kappa_m - [\kappa_{e1}(T) - \kappa_m]p_2}, \tag{17}$$

where $p_1 = (r_1/r_2)^3$, $p_2 = 4\pi {r_2}^3/3a^3$, $v_{1,2} = -1/2 \pm \sqrt{1/4 + 2\kappa_{\theta\theta}/\kappa_{rr}}$, and $w = \sqrt{1 + 8\kappa_{\theta\theta}/\kappa_{rr}}/3$.

Similar to the procedure in two dimensions, the nonlinear modulation is

$$\eta = \frac{81{\kappa_m}^2\kappa_{rr}^2 w^2 p_2 p_1^w}{\left\{\kappa_{rr}(1-p_2)\left[v_1\left(\kappa_c^{(0)} - v_2\kappa_{rr}\right) - v_2\left(\kappa_c^{(0)} - v_1\kappa_{rr}\right)p_1^w\right] + \kappa_m(2+p_2)\left[\left(\kappa_c^{(0)} - v_2\kappa_{rr}\right) - \left(\kappa_c^{(0)} - v_1\kappa_{rr}\right)p_1^w\right]\right\}^2}. \tag{18}$$

Equation (18) is the general expression of nonlinear modulation in three dimensions. Then we will also discuss the nonlinear modulation under thermal coupling conditions.

When the core-shell structure satisfies

$$\kappa_c^{(0)} - v_2\kappa_{rr} = 0, \tag{19}$$

$$\kappa_m = \kappa_c^{(0)}, \tag{20}$$

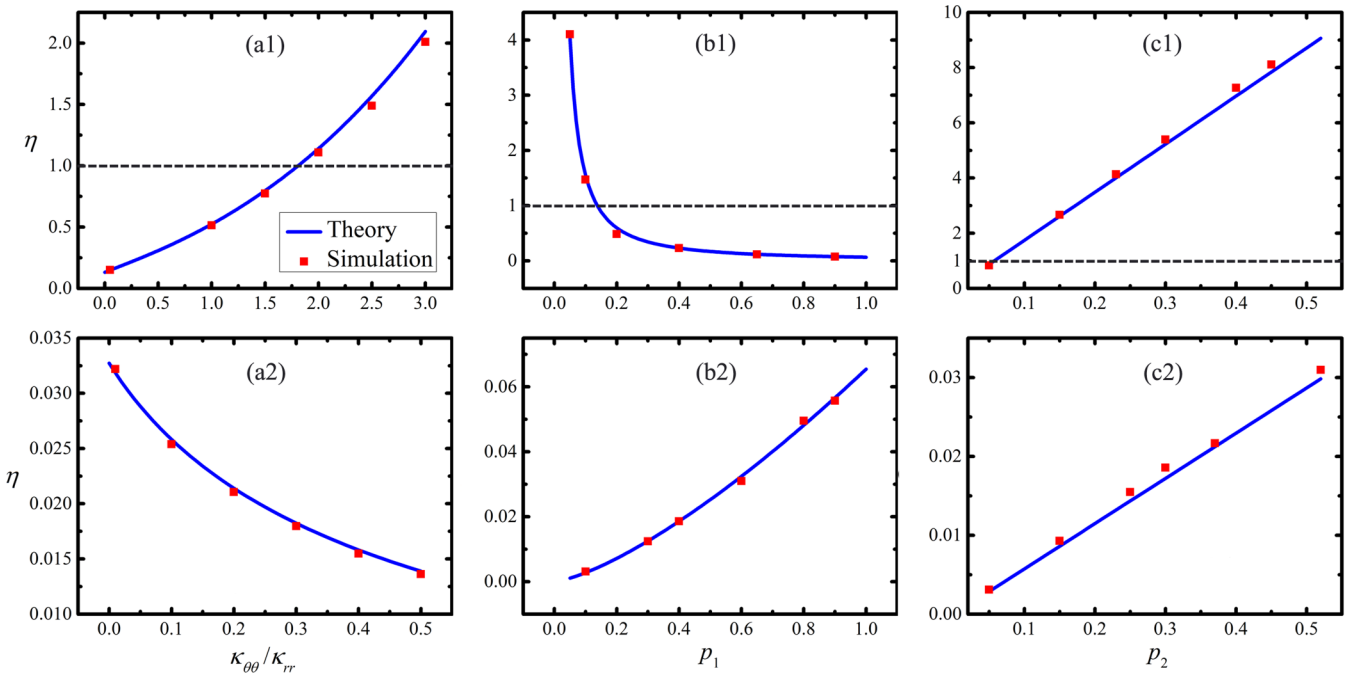

FIG. 3. Three-dimensional simulation results. The solid lines in (a1)–(c1) [or (a2)–(c2)] are calculated from Eq. (21) [or Eq. (24)], and the symbols are obtained from finite-element simulations. Other parameters are the same as those in Fig. 2 except for (a1), (a2) $p_1 = 0.125$ and $p_2 = \pi/48$, (b1), (b2) $\kappa_{\theta\theta}/\kappa_{rr} = 2$ and $p_2 = \pi/48$, and (c1), (c2) $\kappa_{\theta\theta}/\kappa_{rr} = 2$ and $p_1 = 0.125$.

the nonlinear modulation turns to be

$$\eta = p_1^{-w} p_2. \tag{21}$$

On the other hand, when the core-shell structure meets

$$\kappa_c^{(0)} - v_1 \kappa_{rr} = 0, \tag{22}$$

$$\kappa_m = \kappa_c^{(0)}, \tag{23}$$

the nonlinear modulation reaches

$$\eta = p_1^{w} p_2. \tag{24}$$

Similarly, Eqs. (19), (20) and Eqs. (22), (23) are also two different thermal coupling conditions in three dimensions.

III. THEORETICAL CALCULATION VERSUS FINITE-ELEMENT SIMULATION

We have established a theoretical framework to handle the nonlinear modulation (η) in both two and three dimensions, especially under thermal coupling conditions. Now we are in a position to validate the predicted η with finite-element simulations. For this realization, we first calculate the effective thermal conductivity $\kappa_{e2}(T)$ with $J/|\nabla T_0|$, where J is the overall average heat flux obtained from COMSOL MULTIPHYSICS [41]. In Eq. (4), $\kappa_{e2}^{(0)}$ can be theoretically calculated with Eq. (5). T can be approximately regarded as the temperature at the center since the nonlinearity of the system is not that strong. In this way, we can derive η with $[\kappa_{e2}(T) - \kappa_{e2}^{(0)}]/(\chi_c T^\alpha)$ based on finite-element simulations; see symbols in Figs. 2 and 3. Then we explore the nonlinear modulation η when thermal coupling conditions are satisfied, namely, Eqs. (12), (15) for two dimensions and Eqs. (21), (24) for three dimensions in theory; see lines in Figs. 2 and 3.

First we analyze the two-dimensional case whose results are presented in Fig. 2. Figures 2(a1)–2(c1) show the nonlinear modulation under the thermal coupling condition determined by Eqs. (10), (11). According to the theoretical analysis of Eq. (12), the nonlinear modulation is related to three key parameters, say, the degree of shell anisotropy $\kappa_{\theta\theta}/\kappa_{rr}$, the core fraction in the shell p_1, and the core-shell fraction in the matrix p_2. It is noted that the maximum value of p_2 is $\pi/4$ because a circle cannot fill up a square. The nonlinear modulation η can be well manipulated and enhanced under the thermal coupling condition determined by Eqs. (10), (11). Here the word "enhanced" means $\eta > 1$, which indicates that χ_e (effective nonlinear coefficient) is counterintuitively larger than χ_c (the core's nonlinear coefficient). However, the nonlinear modulation η cannot be enhanced (namely, η is always smaller than 1) under the thermal coupling condition determined by Eqs. (13), (14), no matter how one adjusts the three associated parameters.

Then we discuss the three-dimensional case whose results are displayed in Fig. 3. Figures 3(a1)–3(c1) [or Figs. 3(a2)–3(c2)] display the thermal coupling condition determined by Eqs. (19), (20) [or Eqs. (22), (23)]. A similar conclusion can be obtained. That is, only the thermal coupling condition determined by Eqs. (19), (20) succeeds in achieving nonlinearity enhancement (i.e., $\eta > 1$), whereas the thermal coupling condition determined by Eqs. (22), (23) fails.

As shown in Figs. 2 and 3, the finite-element simulation results agree well with the theoretical calculations, and the nonlinearity can be enhanced up to one order of magnitude when the physical parameters are chosen appropriately.

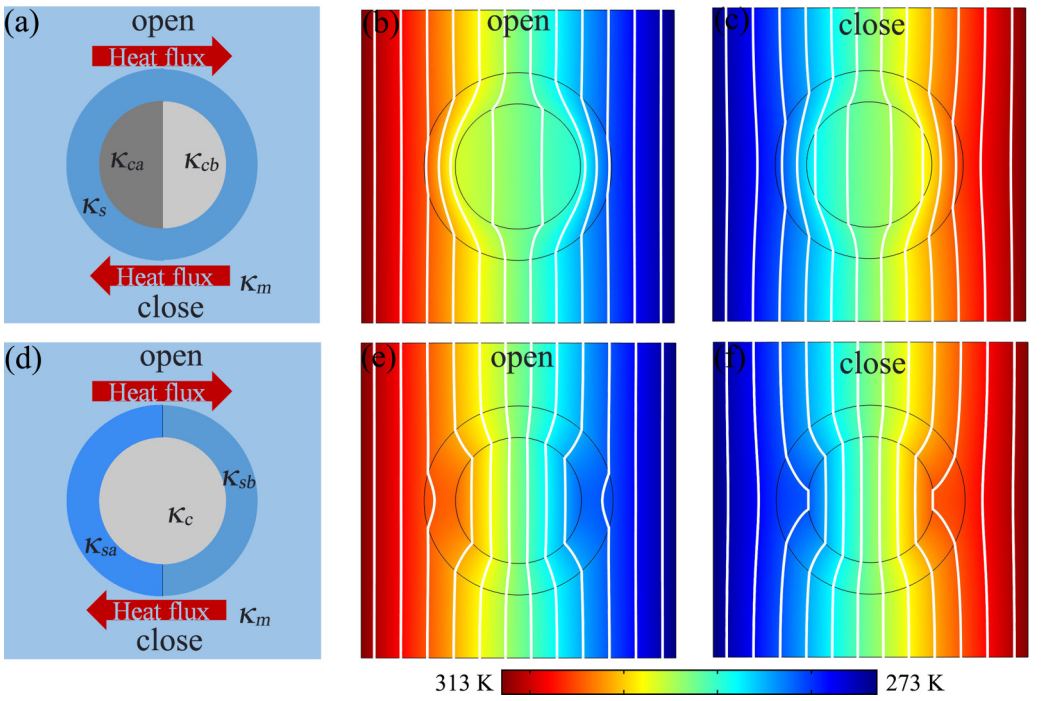

FIG. 4. Switchable thermal transparency device: (a) is the schematic diagram based on the nonlinear core and linear shell and (b), (c) are corresponding finite-element simulation results. (b) is in open state and (c) is in close state. (d) is the schematic diagram based on the linear core and nonlinear shell and (e), (f) are corresponding finite-element simulation results. (e) is in open state and (f) is in close state. Other parameters in (a)–(f): $\kappa_{ca} = 400 + 70 \times (T - 293)$ W/(m K), $\kappa_{cb} = 400 - 70 \times (T - 293)$ W/(m K), $\kappa_s = 100$ W/(m K), $\kappa_c = 20$ W/(m K), $\kappa_{sa} = 400 + 8 \times (T - 293)$ W/(m K), $\kappa_{sb} = 400 - 8 \times (T - 293)$ W/(m K), and $\kappa_m = 200$ W/(m K). Here κ_{ca}, κ_{cb}, κ_{sa}, and κ_{sb} are temperature dependent, which could, in principle, be designed by using shape memory alloys according to the method proposed in Refs. [28,31].

IV. APPLICATION OF NONLINEARITY

In addition, based on the proposed theory, here we design an intelligent (switchable) thermal transparency device; see Fig. 4.

Traditional thermal transparency can ensure the external thermal fields are undistorted [11–16]. However, it is independent of the direction of the thermal fields, which may lack the intelligence for controllability between "open" and "close" state. Here the nonlinear property helps to control the thermal transparency with respect to different directions of the thermal fields, thus being called intelligent thermal transparency.

In Figs. 4(a)–4(c), the device has a nonlinear core and a linear shell. To achieve the effect of switching, here we split the core into two parts. Two kinds of nonlinear thermal

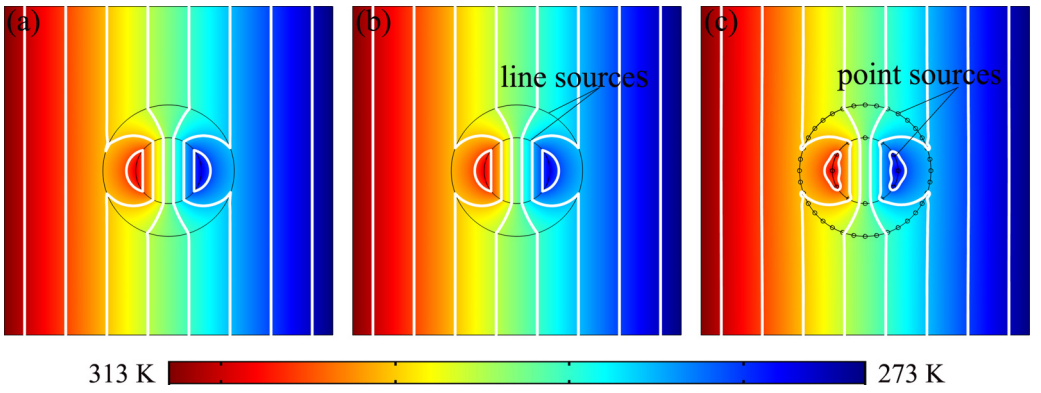

FIG. 5. Replacing (a) apparent negative thermal conductivity with (b) line sources and (c) point sources. The simulation box of (a)–(c) is 16 × 16 cm. The radii of shell r_s and core r_c are 3.2 and 1.6 cm, respectively. The thermal conductivities of background material and core in (a)–(c) are 50 W/(m K). The thermal conductivities of the shells in (a) and (b), (c) are −50 W/(m K) and 20 W/(m K), respectively. Line sources are applied on the two boundaries of the shell in (b). The temperatures of line sources obey $T = 293 - 250 r_{c,s}^2 x/(x^2 + y^2)$ K, where (x, y) represent the Cartesian coordinates whose origin locates in the center of the simulation box. Point sources with radius 0.1 cm are applied on the two boundaries of the shell in (c). The temperatures of point sources can be calculated with $T = 293 - 250 r_{c,s}^2 x/(x^2 + y^2)$ K according to the source positions.

conductivities can respond to different boundary conditions (the direction of heat flux) automatically. When the heat flux goes from left to right [Fig. 4(b)], the temperature is uniformly distributed in the matrix, thus yielding the phenomenon of thermal transparency. In this case, the device is in "open" state; see Fig. 4(b). Conversely, if the heat flux moves from right to left [Fig. 4(c)], the core-shell structure will affect the temperature distribution of matrix, thus eliminating the behavior of thermal transparency. As a result, the device is in "close" state; see Fig. 4(c). Namely, the switching function of the thermal transparency device is achieved as expected.

Also, in Figs. 4(d)–4(f), we design a nonlinear shell and a linear core. Similar results can also be achieved; see Figs. 4(e) and 4(f). A comment on Figs. 4(a)–4(c) and 4(d)–4(f) is that, in spite of the similar switching phenomena, the nonlinearity of the shell [Fig. 4(d)] can be smaller than that of the core [Fig. 4(a)], which means that the manipulation of the shell nonlinearity is more efficient.

V. DISCUSSION AND CONCLUSION

Nonlinearity (namely, thermally responsive thermal conductivity) is of great significance to achieve thermal management. Although natural materials such as copper may exhibit weak nonlinearity, they are still not strong enough to achieve practical nonlinear effects in certain situations. In this work, we have investigated the nonlinear modulation of a core-shell structure embedded in a finite matrix (only the core is nonlinear). Under two thermal coupling conditions, the nonlinear modulation can be largely simplified, and only depends on three key parameters: the degree of shell anisotropy, the core fraction in the shell, and the core-shell fraction in the matrix. Therefore, we can achieve the aim of regulating the nonlinearity by the three tunable parameters. In particular, the nonlinear modulation will be effectively enhanced under the thermal coupling conditions determined by Eqs. (10), (11) and Eqs. (19), (20). Our work lays the foundation for studying the nonlinear property of a core-shell structure, and further work can be expected to explore more complicated cases like nonlinear shells or nonlinear matrices.

In the process of achieving nonlinearity enhancement, apparent negative thermal conductivities [42–45] are applied, which means that the direction of heat flux is from low temperature to high temperature. For this realization, a reliable way is to add external energy to avoid violating the second law of thermodynamics. We also perform finite-element simulations to verify the feasibility of apparent negative thermal conductivities; see Fig. 5. We add external line sources [Fig. 5(b)] and point sources [Fig. 5(c)] on the two boundaries of the shell, and set the thermal conductivity of the shell to be positive. The temperature distributions in Figs. 5(b) and 5(c) are the same as that in Fig. 5(a). Therefore, it is contributing to add external energy. Such point sources can be realized by experiment; see the experimental setup shown in Fig. 1 of Ref. [46].

In summary, this work extends nonlinear research from optics to thermotics, but with essential difference in the definition of nonlinearity [Eq. (1)]. We have proposed a different mechanism to modulate nonlinear thermal responses, and achieved both thermal nonlinearity enhancement and intelligent thermal transparency under various kinds of conditions. We expect that the nonlinearity studied in this work could also have potential applications in heat management including illusion.

ACKNOWLEDGMENT

We acknowledge the financial support by the National Natural Science Foundation of China under Grant No. 11725521.

[1] C. Z. Fan, Y. Gao, and J. P. Huang, Shaped graded materials with an apparent negative thermal conductivity, Appl. Phys. Lett. **92**, 251907 (2008).

[2] T. Y. Chen, C. N. Weng, and J. S. Chen, Cloak for curvilinearly anisotropic media in conduction, Appl. Phys. Lett. **93**, 114103 (2008).

[3] S. Guenneau, C. Amra, and D. Veynante, Transformation thermodynamics: Cloaking and concentrating heat flux, Opt. Express **20**, 8207 (2012).

[4] S. Narayana and Y. Sato, Heat Flux Manipulation with Engineered Thermal Materials, Phys. Rev. Lett. **108**, 214303 (2012).

[5] R. Schittny, M. Kadic, S. Guenneau, and M. Wegener, Experiments on Transformation Thermodynamics: Molding the Flow of Heat, Phys. Rev. Lett. **110**, 195901 (2013).

[6] H. Y. Xu, X. H. Shi, F. Gao, H. D. Sun, and B. L. Zhang, Ultrathin Three-Dimensional Thermal Cloak, Phys. Rev. Lett. **112**, 054301 (2014).

[7] T. C. Han, X. Bai, D. L. Gao, J. T. L. Thong, B. W. Li, and C. W. Qiu, Experimental Demonstration of a Bilayer Thermal Cloak, Phys. Rev. Lett. **112**, 054302 (2014).

[8] Y. G. Ma, Y. C. Liu, M. Raza, Y. D. Wang, and S. L. He, Experimental Demonstration of a Multiphysics Cloak: Manipulating Heat Flux and Electric Current Simultaneously, Phys. Rev. Lett. **113**, 205501 (2014).

[9] S. Guenneau and C. Amra, Anisotropic conductivity rotates heat fluxes in transient regimes, Opt. Express **21**, 6578 (2013).

[10] L. J. Xu, S. Yang, and J. P. Huang, Thermal theory for heterogeneously architected structure: Fundamentals and application, Phys. Rev. E **98**, 052128 (2018).

[11] X. He and L. Z. Wu, Thermal transparency with the concept of neutral inclusion, Phys. Rev. E **88**, 033201 (2013).

[12] L. W. Zeng and R. X. Song, Experimental observation of heat transparency, Appl. Phys. Lett. **104**, 201905 (2014).

[13] T. Z. Yang, X. Bai, D. L. Gao, L. Z. Wu, B. W. Li, J. T. L. Thong, and C. W. Qiu, Invisible sensors: Simultaneous sensing and camouflaging in multiphysical fields, Adv. Mater. **27**, 7752 (2015).

[14] S. Yang, L. J. Xu, R. Z. Wang, and J. P. Huang, Full control of heat transfer in single-particle structural materials, Appl. Phys. Lett. **111**, 121908 (2017).

[15] R. Z. Wang, L. J. Xu, Q. Ji, and J. P. Huang, A thermal theory for unifying and designing transparency, concentrating and cloaking, J. Appl. Phys. **123**, 115117 (2018).

[16] L. J. Xu, S. Yang, and J. P. Huang, Thermal Transparency Induced by Periodic Interparticle Interaction, Phys. Rev. Appl. **11**, 034056 (2019).
[17] T. C. Han, X. Bai, J. T. L. Thong, B. W. Li, and C. W. Qiu, Full control and manipulation of heat signatures: Cloaking, camouflage and thermal metamaterials, Adv. Mater. **26**, 1731 (2014).
[18] T. Z. Yang, Y. Su, W. Xu, and X. D. Yang, Transient thermal camouflage and heat signature control, Appl. Phys. Lett. **109**, 121905 (2016).
[19] Y. Li, X. Bai, T. Z. Yang, H. Luo, and C. W. Qiu, Structured thermal surface for radiative camouflage, Nat. Commun. **9**, 273 (2018).
[20] R. Hu, S. L. Zhou, Y. Li, D. Y. Lei, X. B. Luo, and C. W. Qiu, Illusion thermotics, Adv. Mater. **30**, 1707237 (2018).
[21] S. L. Zhou, R. Hu, and X. B. Luo, Thermal illusion with twinborn-like heat signatures, Int. J. Heat Mass Transfer **127**, 607 (2018).
[22] L. J. Xu, R. Z. Wang, and J. P. Huang, Camouflage thermotics: A cavity without disturbing heat signatures outside, J. Appl. Phys. **123**, 245111 (2018).
[23] L. J. Xu and J. P. Huang, A transformation theory for camouflaging arbitrary heat sources, Phys. Lett. A **382**, 3313 (2018).
[24] K. P. Vemuri and P. R. Bandaru, Anomalous refraction of heat flux in thermal metamaterials, Appl. Phys. Lett. **104**, 083901 (2014).
[25] T. Z. Yang, K. P. Vemuri, and P. R. Bandaru, Experimental evidence for the bending of heat flux in a thermal metamaterial, Appl. Phys. Lett. **105**, 083908 (2014).
[26] K. P. Vemuri, F. M. Canbazoglu, and P. R. Bandaru, Guiding conductive heat flux through thermal metamaterials, Appl. Phys. Lett. **105**, 193904 (2014).
[27] R. S. Kapadia and P. R. Bandaru, Heat flux concentration through polymeric thermal lenses, Appl. Phys. Lett. **105**, 233903 (2014).
[28] Y. Li, X. Y. Shen, Z. H. Wu, J. Y. Huang, Y. X. Chen, Y. S. Ni, and J. P. Huang, Temperature-Dependent Transformation Thermotics: From Switchable Thermal Cloaks to Macroscopic Thermal Diodes, Phys. Rev. Lett. **115**, 195503 (2015).
[29] Y. Li, X. Y. Shen, J. P. Huang, and Y. S. Ni, Temperature-dependent transformation thermotics for unsteady states: Switchable concentrator for transient heat flow, Phys. Lett. A **380**, 1641 (2016).
[30] X. Y. Shen, Y. Li, C. R. Jiang, Y. S. Ni, and J. P. Huang, Thermal cloak-concentrator, Appl. Phys. Lett. **109**, 031907 (2016).
[31] X. Y. Shen, Y. Li, C. R. Jiang, and J. P. Huang, Temperature Trapping: Energy-Free Maintenance of Constant Temperatures as Ambient Temperature Gradients Change, Phys. Rev. Lett. **117**, 055501 (2016).
[32] G. L. Dai, J. Shang, R. Z. Wang, and J. P. Huang, Nonlinear thermotics: Nonlinearity enhancement and harmonic generation in thermal metasurfaces, Eur. Phys. J. B **91**, 59 (2018).
[33] N. A. Nicorovici and R. C. McPhedran, Optical and dielectric properties of partially resonant composites, Phys. Rev. B **49**, 8479 (1994).
[34] O. Levy, Nonlinear properties of partially resonant composites, J. Appl. Phys. **77**, 1696 (1995).
[35] J. P. Huang and K. W. Yu, Enhanced nonlinear optical responses of materials: Composite effects, Phys. Rep. **431**, 87 (2006).
[36] D. H. Liu, C. Xu, and P. M. Hui, Effects of a coating of spherically anisotropic material in core-shell particles, Appl. Phys. Lett. **92**, 181901 (2008).
[37] W. Zhang, M. Ji, and D. H. Liu, Linear and nonlinear properties for a dilute suspension of coated ellipsoids, Phys. Lett. A **373**, 2729 (2009).
[38] W. Zhang and D. H. Liu, Second harmonic generation in composites of ellipsoidal particles with core-shell structure, Solid State Commun. **149**, 146 (2009).
[39] R. C. Zeller and R. O. Pohl, Thermal conductivity and specific heat of noncrystalline solids, Phys. Rev. B **4**, 2029 (1971).
[40] C. J. Glassbrenner and G. A. Slack, Thermal conductivity of silicon and germanium from 3 K to the melting point, Phys. Rev. **134**, A1058 (1964).
[41] http://www.comsol.com/
[42] M. Wegener, Metamaterials beyond optics, Science **342**, 939 (2013).
[43] Y. Gao and J. P. Huang, Unconventional thermal cloak hiding an object outside the cloak, Europhys. Lett. **104**, 44001 (2013).
[44] X. Y. Shen and J. P. Huang, Thermally hiding an object inside a cloak with feeling, Int. J. Heat Mass Tran. **78**, 1 (2014).
[45] L. J. Xu, S. Yang, and J. P. Huang, Designing the effective thermal conductivity of materials of core-shell structure: Theory and simulation, Phys. Rev. E **99**, 022107 (2019).
[46] D. M. Nguyen, H. Y. Xu, Y. M. Zhang, and B. L. Zhang, Active thermal cloak, Appl. Phys. Lett. **107**, 121901 (2015).